

CONSTRAINTS FROM ROCKS IN THE TAIWAN OROGEN ON CRUSTAL STRESS LEVELS AND RHEOLOGY

Steven Kidder¹, Jean-Philippe Avouac¹, Yu-Chang Chan²

¹California Institute of Technology, ²Academia Sinica

ABSTRACT

Taiwan's Hsuëhshan range experienced penetrative coaxial deformation within and near the brittle-plastic transition between 6.5 Ma and 3 Ma. This recent and short-lasting deformation in an active, well-studied orogen makes the Hsuëhshan range an ideal natural laboratory for studying the rheology of crustal materials. We apply recrystallized grain size piezometry here for the first time in a setting where multiple comparisons can be made with independent constraints on stress. Grain size piezometry results are paired with Titanium-in-quartz thermobarometry and other temperature constraints and give peak differential stresses at the brittle-ductile transition ($T = 250\text{--}300^\circ\text{C}$) of ~ 200 MPa that taper off to ~ 80 MPa at $\sim 350^\circ\text{C}$. Earlier deformation at temperatures $\sim 350\text{--}500^\circ\text{C}$ occurred at stresses ~ 14 MPa. Results are not strongly dependent on the setting in which quartz is found (e.g. in veins vs. quartzite). Given tight geodetic and structural constraints on strain rate, we show that our stress estimates are consistent with widely applied quartzite flow laws, potential energy constraints based on topography, Byerlee's rule and Goetze's criteria. The agreement between our results and these independent estimates supports the use of the recrystallized grain size piezometer, a quick and inexpensive method for resolving stress histories in exhumed rocks. Consideration of the various stress estimates indicates an integrated crustal strength of $1.5\text{--}2.1 \times 10^{12}$ N/m, consistent with a weak strength-depth profile and friction coefficient within the Taiwan wedge of ~ 0.38 .

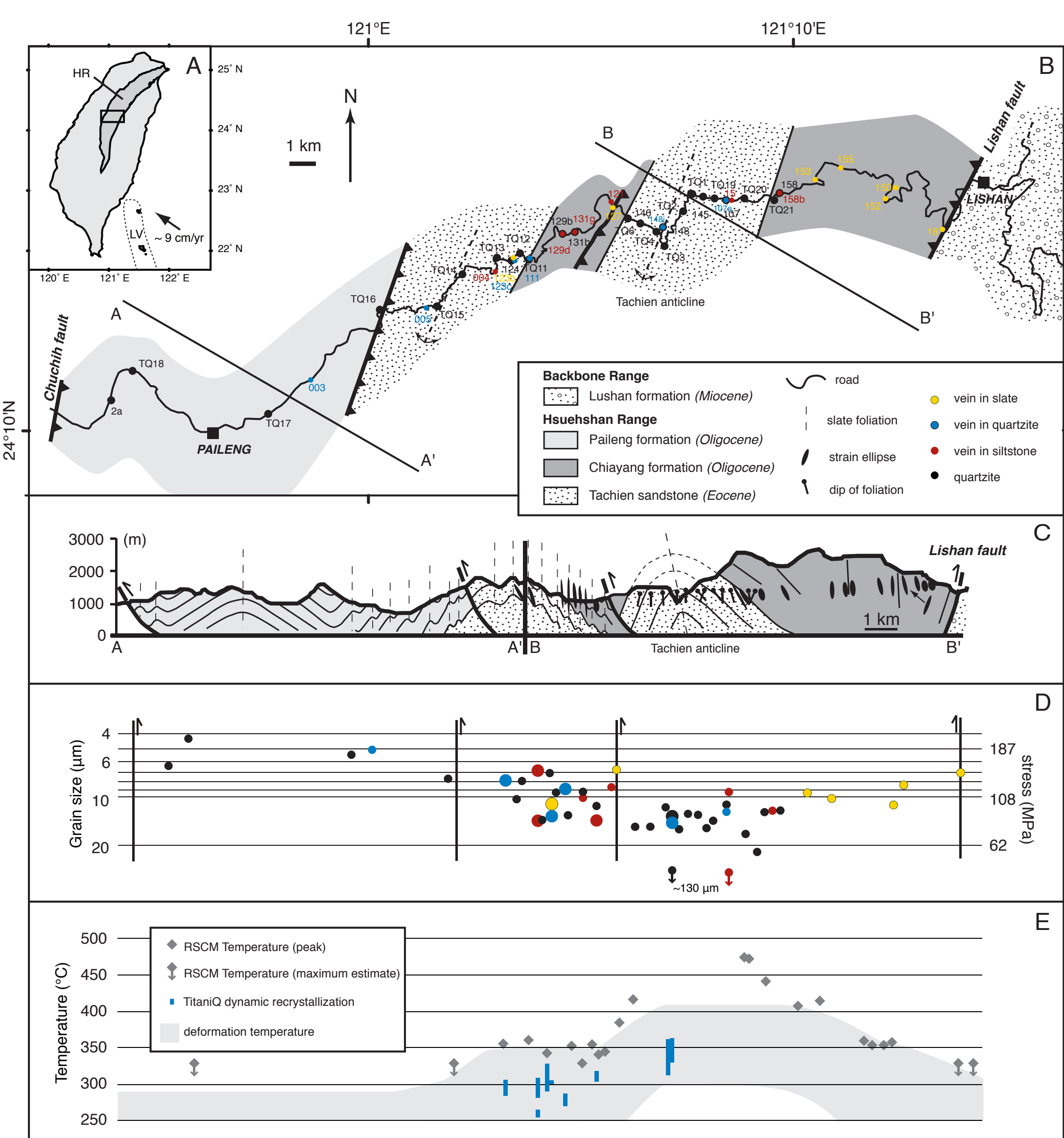


Figure 1. A: Map of Taiwan showing the Hsuëhshan range (HR), Luzon volcanic arc (LV), study area and plate convergence vector (e.g. Gueydan, 2003). B: Map of the study area showing sample localities and major structures. C: Cross section showing major structures, foliation measurements, strain ellipses in slate (Tillman and Byrne, 1995), and our foliation measurements in quartzite. D: Grain size data and corresponding stress estimates plotted relative to position on cross section. Data points associated with good temperature constraints are enlarged. E: Summary of temperature constraints. Raman spectroscopy of carbonaceous material ("RSCM," Beysac et al.) serves as a peak temperature constraint; titanium-in-quartz temperature estimates are deformation temperatures. The grey-shaded field summarizes deformation-temperature constraints for late deformation.

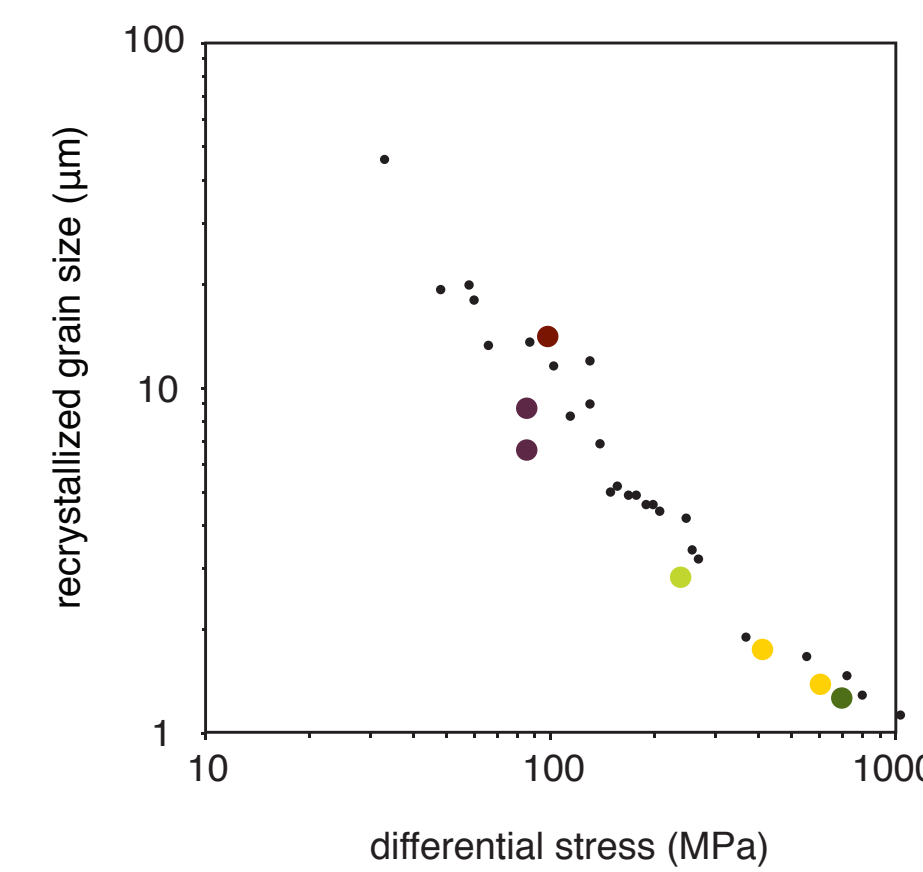


Figure 2. Experimental data for quartz showing relationship between recrystallized grain size and differential stress. Experiments were carried out between 700 and 1200 degrees.

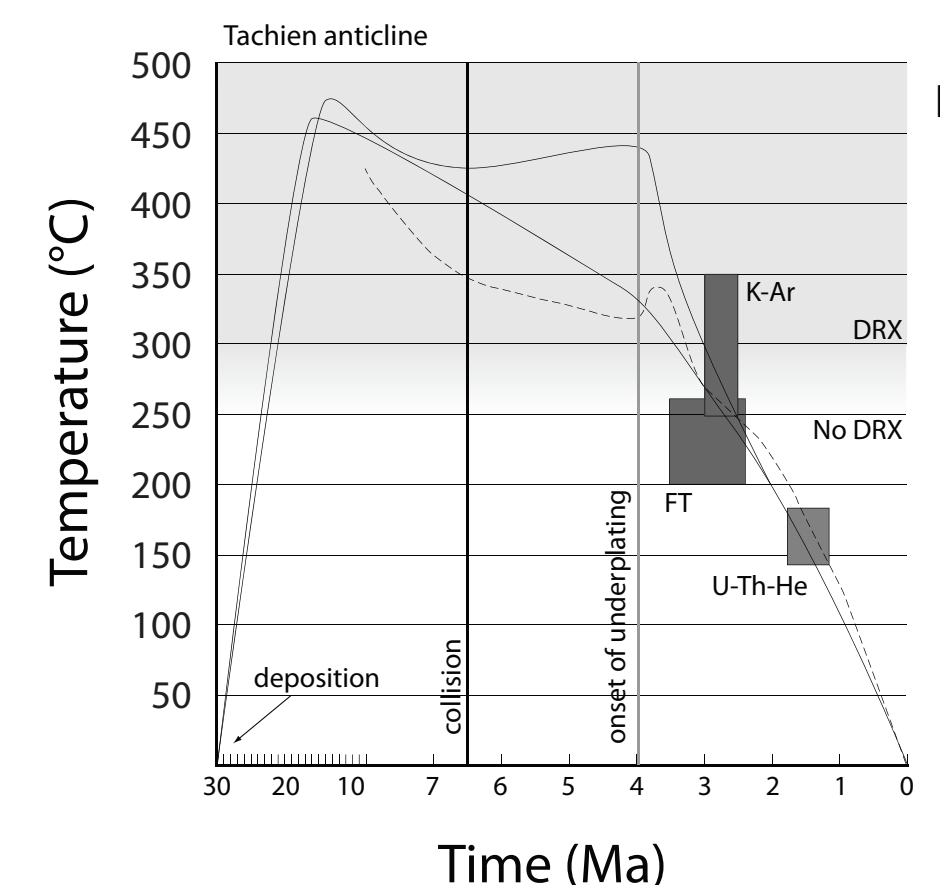


Figure 3. Constraints on temperature-time history and possible cooling paths for the deepest exposed levels of the Hsuëhshan range where quartzites and one vein were sampled. Dashed line from thermal-kinematic model of Simoes et al. (2007). The thin black lines represent alternative cooling paths constrained by evidence of elevated temperatures at the onset of collision. Grey and white fields separate regions where dynamic recrystallization (DRX) occurs (grey) or does not occur (white).

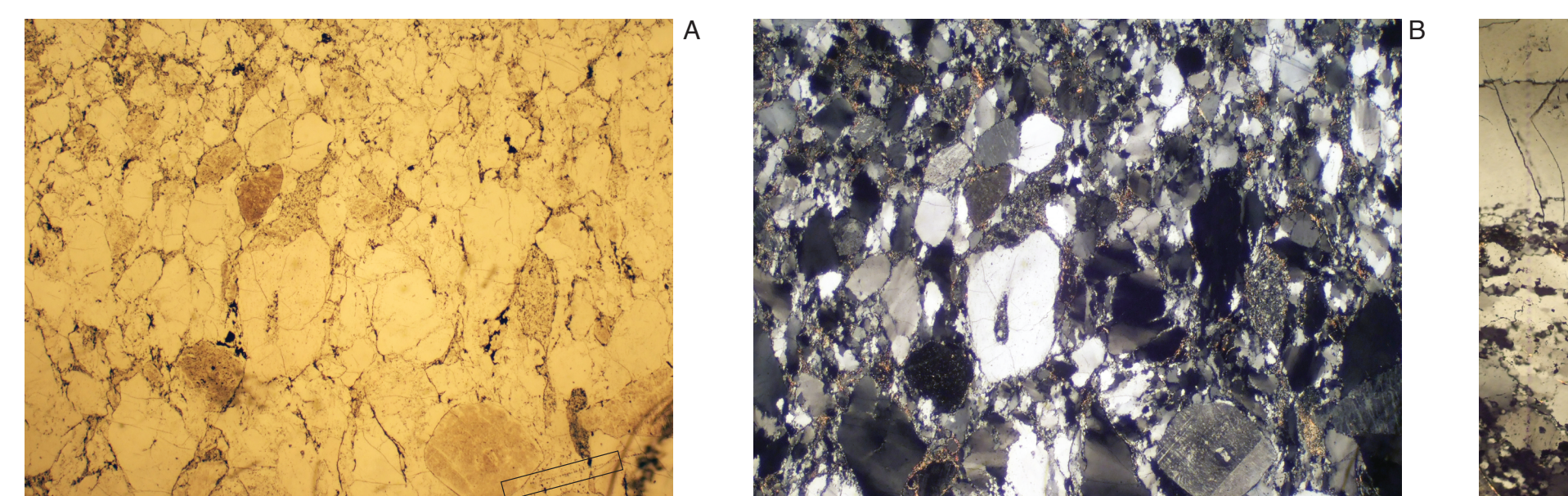


Figure 4. Photomicrographs of quartzite sample 148d. A: unpolarized. B: Cross polarized. Location of C in lower right. Bedding is horizontal. FOV ~ 7 mm. C: close up showing recrystallized grains.



Figure 5. Vein swarm from the core of a small anticline (sample 004). Multiple generations of veins crosscut one another. Many veins are dynamically recrystallized (see figure 6). Recrystallized grain size reflects stress conditions at the brittle-ductile transition. Titanium-in-quartz thermometry indicates vein emplacement at $260\text{--}300^\circ\text{C}$.

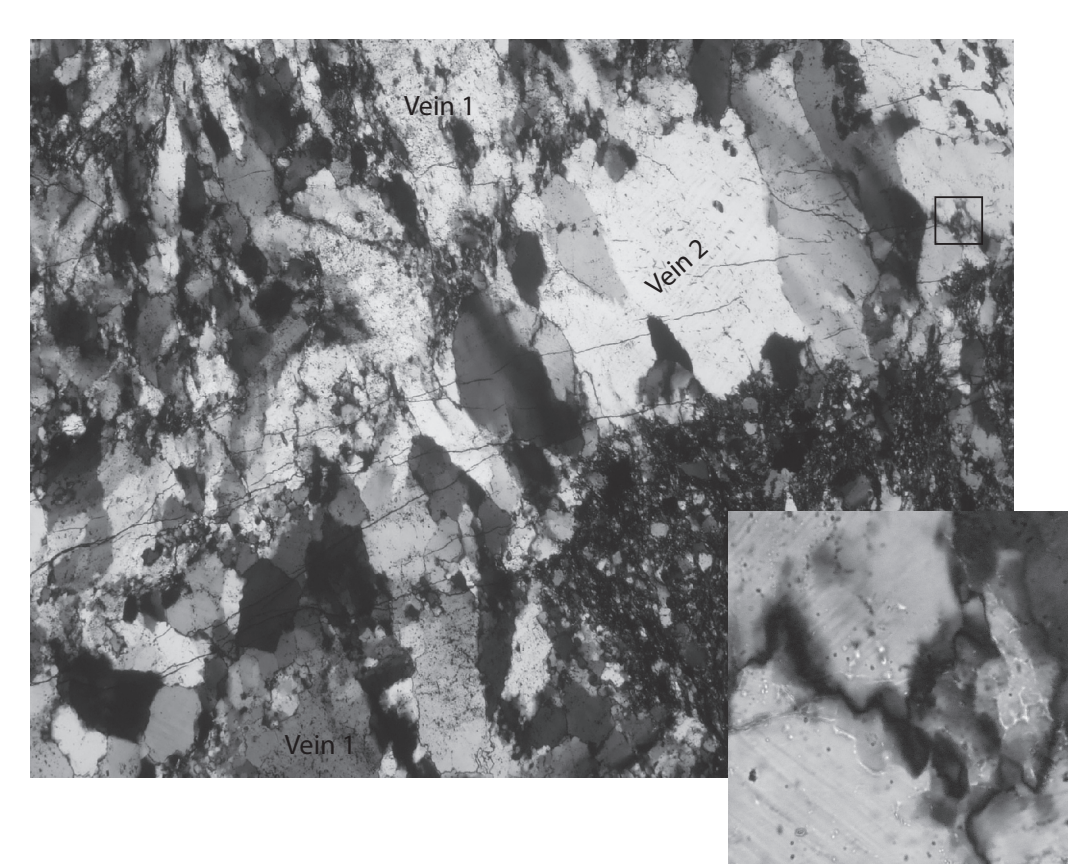


Figure 6. Petrographic evidence of deformation within the brittle-ductile transition (sample 004). Given the temperature-time paths in figure 3, microstructural constraints shown here demonstrate that vein emplacement occurred above 250°C (the minimum temperature for dynamic recrystallization of quartz). Early vein material is strongly recrystallized. A late vein running from lower left to upper right postdates dynamic recrystallization of the earlier vein. The late vein has a lower inclusion concentration and retains some crystal facets (lower left). Undulatory extinction, subgrains, and minor dynamic recrystallization (inset) of the late vein indicate it too was deformed at temperatures $>250^\circ\text{C}$. FOV ~ 2.7 mm.

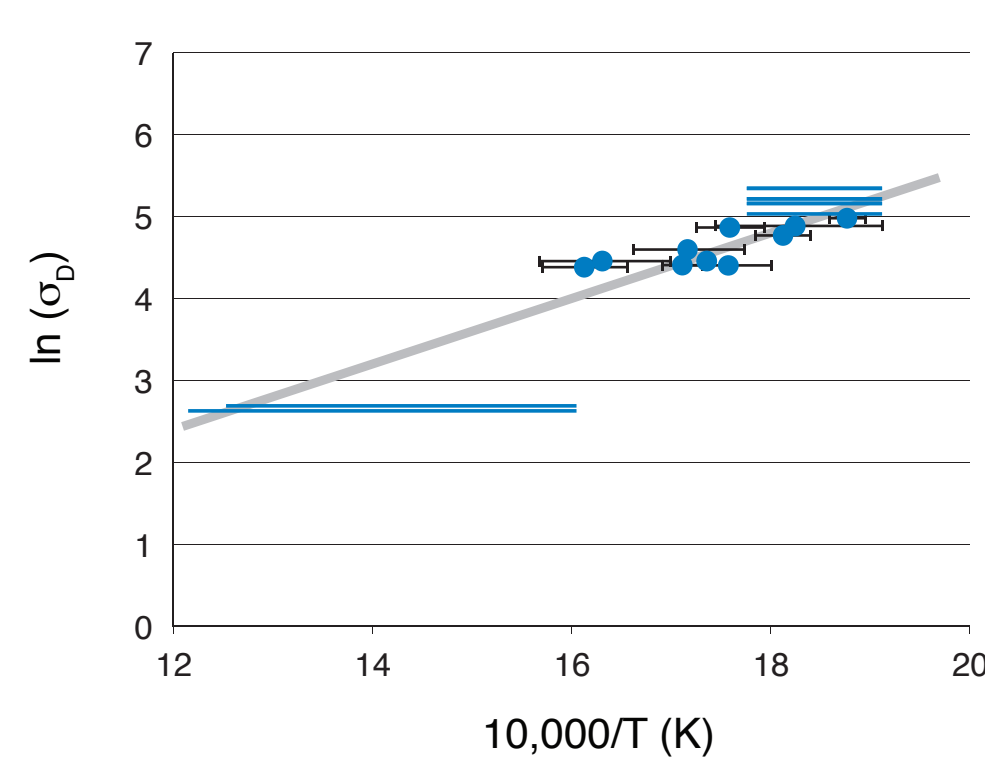


Figure 7. Arrhenius plot showing our temperature and stress data. The line shown has the minimum slope given the data constraints. Theory and experimental observations (Poirier, 1985), indicate that dislocation creep in quartz deformation follows a flow law of the form:

$$\dot{\epsilon} = A \sigma^n e^{-Q/RT}$$

where A is material constant dependent on water fugacity, Q is the creep activation energy (kJ mol⁻¹), R is the gas constant, T is absolute temperature, and σ is differential stress. The equation can be reformulated as:

$$\ln(\sigma) = B + Q/nRT$$

where B includes A , n and $\dot{\epsilon}$. Stress and temperature data graphed on a plot of $\ln(\sigma)$ vs. $1/T$ have a slope of Q/nR . Assuming a stress exponent of $n=4$, the slope corresponds to a minimum activation energy of 133 kJ/mol (experimental values are 134-279). This observation validates the extrapolation of experimental quartz results from high-temperature laboratory experiments to geologic conditions because it suggests that the same deformation processes are responsible for deformation in both the lab and nature. If a different process began to dominate at low temperatures, it should have a lower activation energy than the experimental value.

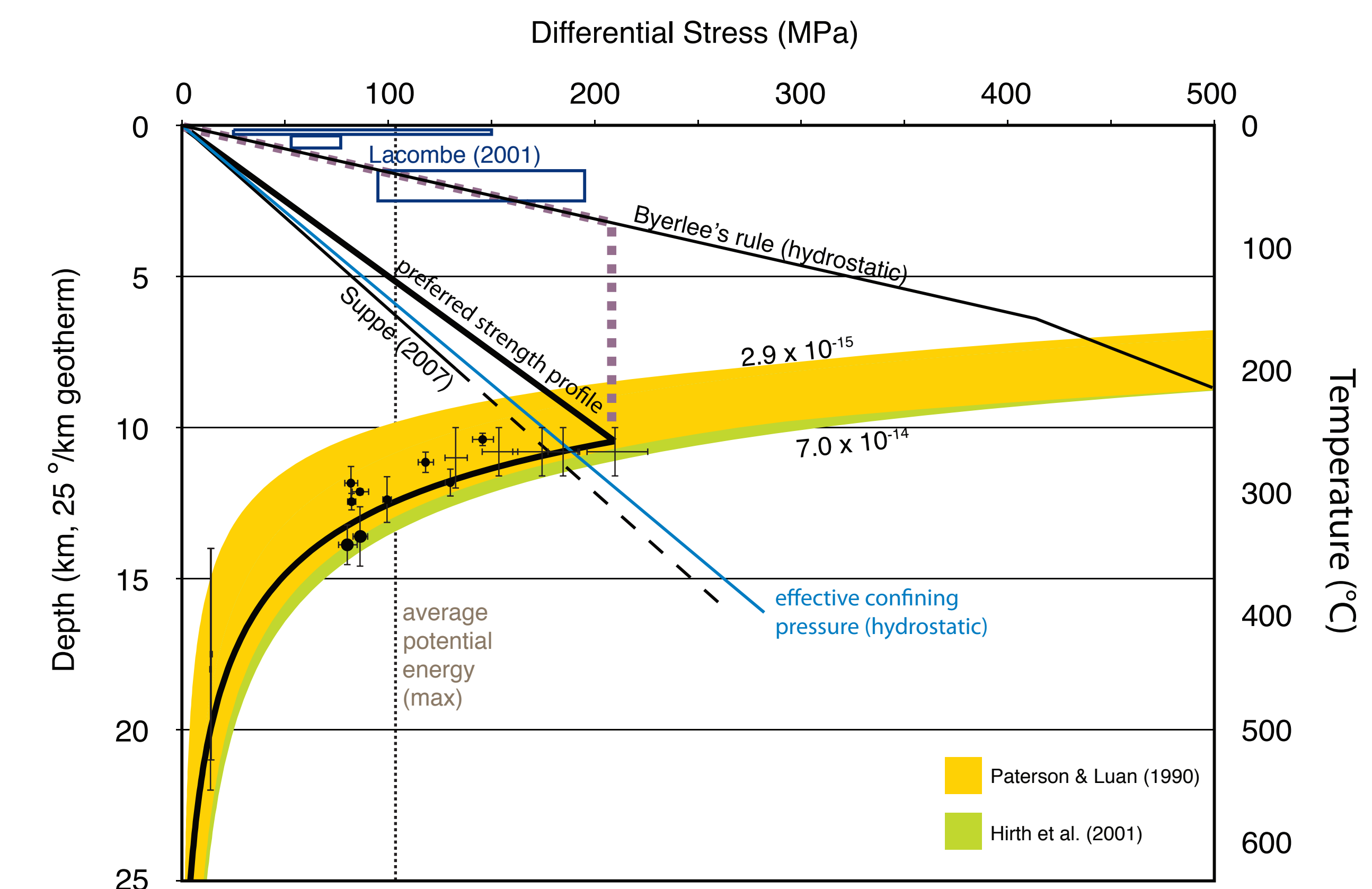


Figure 8. Stress-depth diagram showing results (2σ standard errors) for samples with good temperature constraints. Also shown are predictions of widely used flow laws plotted over the window of permissible strain rates calculated for samples from the Tachien anticline (the two larger black circles, critical taper results from Suppe 2007, calcite twin results from Lacombe (2007). Our preferred strength envelope is shown as a thick black line. The dotted purple line shows the upper part of an alternative strength profile following a strict interpretation of Byerlee's rule.

CONCLUSIONS

- 1) The recrystallized grain size piezometer in quartz produces stress estimates at the brittle-ductile transition consistent with multiple independent constraints including widely applied quartzite flow laws, critical taper, potential energy estimates resulting from elevation differences, Byerlee's rule and Goetze's criteria. Accuracy is probably better than a factor of two.
- 2) The activation energy of naturally deformed quartzite is >133 kJ/mol, consistent with experimental determinations.
- 3) Peak differential stress in the Hsuëhshan range was ~ 210 MPa. Our results indicate hydrostatic fluid pressure and a low friction coefficient within the Taiwan wedge of ~ 0.38 . Integrated crustal strength in Taiwan is $1.5\text{--}2.1 \times 10^{12}$ N/m.
- 4) Strain-weakening, rather than extreme fluid pressure, is likely responsible for low stresses at deep levels on major faults in Taiwan.